Progress In The Growth Of Mid-Infrared InAsSb Emitters By Metal-Organic Chemical Vapor Deposition

R. M. Biefeld *, A. A. Allerman, S. R. Kurtz, and K. C. Baucom
Sandia National Laboratory, Albuquerque, New Mexico, 87185-0601, USA

ABSTRACT

We report on recent progress and improvements in the metal-organic chemical vapor deposition (MOCVD) of mid-infrared InAsSb emitters using a high speed rotating disk reactor (RDR). The devices contain AlAsSb claddings and strained InAsSb active regions. These emitters have multi-stage, type I, InAsSb/InAsP quantum well active regions. A semi-metal GaAsSb/InAs layer acts as an internal electron source for the multi-stage injection lasers and AlAsSb is the electron confinement layer. These structures are the first MOCVD multi-stage devices. Growth in an RDR was necessary to avoid the previously observed Al memory effects found in a horizontal reactor. Broadband LED's produced 2 mW average power at 3.7 μm and 80 K and 0.1 mW at 4.3 μm and 300K. A multi-stage, 3.8-3.9 μm laser structure operated up to T=180 K. At 80 K, peak-power > 100 mW/facet and a high slope-efficiency (48%) were observed in these gain guided lasers.

Key Words: InAsSb IR Emitters, Mid-Infrared Lasers, MOCVD, Multi-stage lasers

PACS Numbers: 81.15.Gh, 42.55.P

* Phone 505-844-1556, Fax 505-844-1556, email rmbiefe@sandia.gov

DISCLAIMER

INTRODUCTION

Mid-infrared (3-6 μm) lasers and LED's are being developed for use in chemical sensor systems and infrared countermeasure technologies. These applications require relatively high power, mid-infrared lasers and LED's operating near room temperature. The radiative performance of mid-infrared emitters has been limited by non-radiative recombination processes (usually Auger recombination) in narrow bandgap semiconductors. Potentially, Auger recombination can be suppressed in "band-structure engineered", strained, Sb-based heterostructures. We have demonstrated improved performance for midwave infrared emitters in strained InAsSb heterostructures due to their unique electronic properties that are beneficial to the performance of these devices.[1-3] We are exploring the growth by metal-organic chemical vapor deposition (MOCVD) of novel, multi-stage (or "cascaded") active regions in InAsSb-based devices, to further improve laser and LED performance.

Multi-stage, mid-infrared gain regions have been proposed for several material systems.[1-6] Ideally, a laser with an N-stage active region could produce N photons for each carrier injected from the external power supply. Multi-staging of the laser active region may increase gain, lower threshold current, and finally increase the operating temperature of gain-limited, mid-infrared lasers. The success of the unipolar, quantum cascade laser demonstrates the benefit of multi-stage gain regions.[7] Gain regions with multiple electron-hole recombination stages have been proposed for Sb-based lasers.[1,5,6] Recently, cascaded lasers with type II InAs/GaInSb active regions have been

demonstrated.[8] These type II lasers were grown by molecular beam epitaxy, and, characteristic of multi-stage lasers, differential quantum efficiencies exceeding one are now reported.[9] In this work we demonstrate 10-stage lasers with InAsSb quantum wells and type I band offsets and differential quantum efficiencies exceeding one .

A band diagram of a single stage in our multi-stage active region, under forward bias, is shown in Figure 1. Electron-hole recombination occurs in compressively strained InAsSb quantum wells separated by tensile strained InAsP barriers. Electron-hole pairs for each stage are generated at a semi-metal, GaAsSb (p)/ InAs (n) heterojunction. An AlAsSb layer prevents electrons from escaping; nominal hole confinement is provided by the InAsSb quantum well valence band offset relative to the InAsP barrier layer in this initial device. Ideally, electron-hole generation replenishes the carriers which recombine in each stage, and for each carrier injected from the external circuit, the multi-stage active region can emit several photons resulting in an overall quantum efficiency greater than unity. Previously, we have found that a AlGaAsSb graded layer between the AlAsSb and GaAsSb layers reduces hole trapping, thus increasing laser duty cycles and lowering turn-on voltages.[10] We have observed similar improvements in devices containing either a heavily doped GaAsSb/AlAsSb interface or a GaAsSb/AlAsSb short period superlattice.

Unlike previous cascaded lasers and LED's[4-9] our device was grown by MOCVD. Our devices are among the most complex structures ever grown by MOCVD, and it can be difficult to alternate Al, In, Ga, P, As, or Sb bearing materials while maintaining sharp interfaces and managing chemical carry-over into other layers. We have found that the combination of novel Al organometallic sources and an MOCVD, vertical, high speed

rotating-disk reactor (RDR) is necessary to grow these structures to avoid the chemical carry-over previously observed with a horizontal reactor.[3] Even with an RDR, it is necessary to optimize the growth conditions and the reactor configuration as discussed below to minimize the possibility of chemical carry over.

EXPERIMENTAL

This work was carried out in a previously described vertical, high-speed, rotating-disk reactor (RDR).[11] Ethyldimethylamine alane (EDMAA), trimethylindium (TMIn), triethylgallium (TEGa), triethylantimony (TESb) , diethylzinc (DEZn), phosphine, and tertiarybutylarsine (TBAs) or arsine were used as sources. P-type doping was accomplished using diethylzinc (DEZn) in a dilution system. The structures were grown at 500 ^{0}C and 70 torr. The V/III ratios were optimized separately for each material and the InAsSb/InAsP strained-layer superlattice. Hydrogen was used as the carrier gas at a flow of 18.5 slpm with a substrate rotation speed of 1500 rpm to retain matched flow conditions.[11] Semi-insulating, epi-ready (001) GaAs for Hall samples or n-type (001) InAs substrates were used for each growth.

Both InAsSb/InAs and InAsP/InAs multiple quantum wells (MQWs) were grown for calibration purposes to determine the solid-vapor distribution coefficients separately for Sb in InAsSb and P in InAsP. The InAsSb/InAsP SLSs were lattice matched to InAs with a mismatch < 0.0004. The MQW and SLS composition, layer thicknesses, and strain were determined by double crystal x-ray diffraction (DCXRD). DCXRD was also used to determine alloy composition. Alloy layer thicknesses were determined using a

groove technique and these were checked in several instances by cross sectional SEM. These techniques agreed to within a few percent.

Infrared photoluminescence (PL) was measured on all samples at 14 K and 300 K using a double-modulation, Fourier-transform infrared (FTIR) technique. This technique provides high sensitivity, reduces sample heating, and eliminates the blackbody background from infrared emission spectra. Injection devices also were characterized with double modulation FTIR.

RESULTS AND DISCUSSION

MOCVD Growth

The best growth conditions found in this investigation for $AlAs_xSb_{1-x}$ occurred at 500 °C and 70 torr at a growth rate of 3.2 Å/s using a V/III ratio of 5.3. The 5/3 ratio was calculated using a vapor pressure of 0.75 torr for EDMAA at 19.8 °C and an [TESb]/([TBAs]+[TESb]) ratio of 0.83. The growth rate was found to be dependent on the EDMAA flow and independent of the group V flows for the conditions examined in this work. The best surface morphologies with the lowest number of defects were obtained by using a buffer layer grown before the $AlAs_xSb_{1-x}$ layer. The defects consisted primarily of square pyramidal hillocks 10 to 20 μm on a side. Lattice matched $AlAs_xSb_{1-x}$ films of high crystalline quality, as evidenced by DCXRD where full widths at half of the maximum intensity (FWHM) of 27 to 50 arc seconds were obtained. Typical InAs substrate peaks were 10-20 arc seconds. The x-ray peak width of 50 arc seconds could be due to some variation in composition with growth time as discussed below or to phase

separation. We were also able to reproducibly obtain lattice matching of $AlAs_xSb_{1-x}$ to InAs to within less than 0.015 percent using the optimized growth conditions. Figure 2 shows the variation of lattice mismatch from the InAs substrate or composition as a function of TBAs flow for the optimized growth conditions. This variation was reproducible at these growth conditions. Hall measurements of AlAsSb films 1 μm thick with 200Å GaAsSb cap layers grown on GaAs substrates indicated background hole concentrations between 0.5 to 1 $x10^{17}$ cm^{-3}. The residual hole concentration of GaAsSb films on GaAs ranged between 4 to $7x10^{16}$ cm^{-3}. The use of other than the above stated growth conditions led to several significant problems during the growth of $AlAs_xSb_{1-x}$ layers lattice matched to InAs. These included composition control and reproducibility. For instance, growth at higher V/III ratios resulted in a large drift in composition from run to run and broad x-ray diffraction peaks. Composition variations have also been observed due to excess cooling of the chamber walls due to an Sb memory effect on the inlet to the reactor.

We have successfully doped the $AlAs_xSb_{1-x}$ layers p-type using DEZn. We achieved p-type levels of 1 x 10^{16} to 6 x 10^{17} cm^{-3}. The mobilities for the $AlAs_xSb_{1-x}$ layers ranged from 200 to 50 cm^2/Vs with no clear trend that could be associated with the carrier concentration or type. The Zn doping levels were determined from Van der Pauw/Hall measurements and confirmed by secondary ion mass spectroscopy (SIMS) on thick calibration samples. SIMS measurements on the Zn doped samples indicated a similar level of Zn compared to the p-type carriers indicating complete activation of the Zn. Two orders of magnitude higher DEZn partial pressures were required to obtain

equivalent dopant levels in $AlAs_{0.16}Sb_{0.84}$ compared to $GaAs_{0.09}Sb_{0.91}$. This lower incorporation rate for Zn in AlAsSb indicates a possible depletion reaction between DEZn and EDMAA.

Growth rates of 2.8 Å/s were used for the growth of InAsSb/InAs and InAsP/InAs MQW structures. The growth rate was found to be proportional to the TMIn flow into the reaction chamber and independent of the group V flows. A purge time of 15 to 20 seconds with arsine flowing during the purge was used between InAs and the ternary layer growth to allow for source flow changes during the growth of the MQWs. Figure 3(a) illustrates the dependence of Sb composition on the TESb/(TESb+TBAs) vapor phase composition for optimized growth conditions. In this set of experiments the flow of TESb was held constant while the TBAs flow was varied to change the Sb solid composition. The V/III ratio varied from 1.9 to 5.9. A low V/III ratio is necessary for the growth of high quality InAsSb due to the low vapor pressure of Sb; excess Sb tends to cause surface morphology defects. In Figure 3(b) the dependence of P composition in InAsP on the variation of TBAs/(TBAs + Phosphine) vapor phase composition is illustrated. The flow of phosphine was held constant and the flow of TBAs was varied. In this case the V/III ratio is dominated by the excess phosphine flow and was approximately constant at 70. The high V/III ratio and excess phosphine flow are necessary because of the high decomposition temperature of phosphine. In both cases, InAsSb/InAs and InAsP/InAs, the composition dependence was reproducible and approximately linear over the composition range that was examined.

Several test laser structures were prepared similar to the one previously reported using InAsSb/InAs MQW active regions.[3] These structures consisted of 2 μm p-type AlAsSb top and bottom cladding layers with InAsSb/InAs 10 period MQW active regions and a (p)-GaAsSb/(n)-InAs semi-metal heterojunction for charge transfer. [1-3] The difference in the quality of the x-ray diffraction pattern of the continuously grown structure from the RDR and the re-grown active region and top cladding is illustrated in Figure 4. The continuously grown structures can be seen to be of much better quality from the x-ray diffraction pattern (top pattern). Similar lasing characteristics were obtained for both the RDR and re-grown structures. The advantage of the RDR growths is that no Al carry-over was observed as was found for the structures grown using the horizontal reactor without re-growth.[3] The multi-staged laser structures described in this paper would be impractical to grow using the re-growth technique developed in our conventional horizontal MOCVD system.

The growth of the InAsSb/InAsP ternary strained-layer superlattices (SLSs) used similar conditions as those for the MQW growths. The growth conditions for a given composition of the SLS was easily predicted from the compositions of the MQW's. However, very rough surface morphologies and poor x-ray diffraction patterns and photoluminescence characteristics were found for the 15-20 second purge times used between layers. The purge times were optimized using both x-ray diffraction patterns, as illustrated in Figure 5, as well as photoluminescence. As shown in Figure 5(a) and (b) for purge times of 20 and 5 seconds, very broad x-ray diffraction patterns were observed. The x-ray diffraction patterns shown in Figure

5(c) and (d) differ only in composition; both were grown using no purges between layers. The sample in (d) was grown with a slightly different composition to achieve lattice matching with the InAs substrate. Similar characteristics were found for purge times of 0 or 1 second with arsine continuing to flow during the purge times as well as during the growth of the layers.

10-Stage, Cascaded InAsSb Quantum Well LED's and Lasers at 3.9 μm

We have prepared ten-stage, cascaded InAsSb quantum well lasers. Each stage consisted of a $GaAs_{0.09}Sb_{0.91}$ (p, 300 Å) /InAs (n, 500 Å) semi-metal , 3 or 5 $InAs_{0.85}Sb_{0.15}$ (n, 94 Å) quantum wells separated by 4 $InAs_{0.67}P_{0.33}$ (n, 95 Å) barriers, an $AlAs_{0.16}Sb_{0.84}$ (p, 50 Å) electron block, a compositionally graded, Zn-doped AlGaAsSb ($p = 5 \times 10^{17}$ cm^{-3} , 300 Å) layer and a final 50 Å, Zn-doped $GaAs_{0.09}Sb_{0.91}$ layer. The total thickness of the gain region is 1.9 μm. The excellent crystalline quality of these laser structures is demonstrated in the x-ray diffraction spectrum of the 5 well active region where groups of satellite peaks corresponding to a gain-stage period of 2100 Å and the InAsSb/InAsP period of 190 Å are observed as illustrated in Figure 6. The composition and layer thickness for the InAsSb/InAsP superlattice can be determined from the satellites with the large repeat distance where the smaller repeat distance as shown in the inset is determined by the 10-stage structure.

Optical confinement for these lasers is provided by 2 μm thick , Zn-doped $AlAs_{0.16}Sb_{0.84}$ ($p=1 \times 10^{17} cm^{-3}$) claddings on both sides of the active region. A top 1500 Å Zn-doped $GaAs_{0.09}Sb_{0.91}$ layer ($p=2 \times 10^{18}$ cm^{-3}) is used as a contact and protective

layer. The structure is lattice matched to the InAs substrate. An InAs (n, 500 Å) /$GaAs_{0.09}Sb_{0.91}$ (p, 1000 Å) semi-metal is used to enable carrier transport from the n-type InAs substrate into the p-type $AlAs_{0.16}Sb_{0.84}$ cladding layer.

Narrow LED and photoluminescence emission peaks of the 10-stage laser wafers indicated good stage-to-stage uniformity of the InAsSb/InAsP multiple quantum wells. Only InAsSb/InAsP emission was observed in the LED spectrum. Emission from the InAs layer would be a strong indication of inadequate carrier confinement in the InAsSb quantum wells. The LED emission wavelength shifted from 3.7 μm (80 K) to 4.3 μm (300 K) due to the temperature dependence of the InAsSb/InAsP bandgap. Operated at 50% duty cycle, average LED output powers were 2.4 mW at 80 K and 100 μW at 300 K when driven with 200 mA average current. We speculate that the rapid decrease in LED power with temperature is due to thermal emission of holes from the InAsSb/InAsP quantum wells.

Lasing was observed from gain-guided stripe lasers. The facets were uncoated, and stripes were indium soldered to the heat sink with the epitaxial side up. Under pulsed operation with 100 nsec pulses at 1 kHz (10^{-4} duty-cycle), stimulated emission was observed from 80-180 K and 3.8 to 3.9 μm. Laser emission spectra at 80 K and 150 K are shown in Figure 7. For 500 μm long stripes with 80 μm wide metallizations, several longitudinal modes are observed with a mode spacing of 2.7 cm^{-1}. The longest laser pulses were 1 μsec. These initial devices were easily damaged by increased heating associated with higher temperature operation or longer duty cycles. Threshold current densities for these 10-stage devices were = 1 kA/cm^2. Lower threshold current densities (

0.1 kA/cm^2) have been demonstrated in single-stage, type I mid-infrared lasers at 80 K.[12] The T_0 of the 5-well laser was 34 K which is similar to our previously reported, optically pumped and injection InAsSb/InAsP lasers.[2]

The laser output was collected and focused directly onto an InSb detector to obtain power-current data. At 80 K, peak power values > 100 mW/facet were obtained. The maximum slope-efficiency was 150 mW/A, corresponding to a differential external quantum efficiency of 48 % (4.8 % per stage). This initial result is promising when compared to the value obtained for a second generation, 23-stage type II cascaded laser (3.9 μm) with a differential quantum efficiency of 131% (5.7 % per stage).[9] The slope-efficiency was strongly dependent on cavity length, and analysis of efficiency data suggest an internal quantum efficiency > 1 and a loss coefficient = 100 cm^{-1}.[10]

SUMMARY

In conclusion, we have demonstrated the first cascaded lasers and LED's with type I InAsSb quantum well active regions grown using MOCVD. Also, these are the first cascaded devices grown by MOCVD. The 10-stage, 3.8-3.9 μm laser operated up to 180 K. At 80 K, peak laser power > 100 mW/facet and a slope-efficiency of 48% (4.8% per stage) were observed with internal quantum efficiencies > 1. We are optimistic that advances in material quality and device design will improve carrier confinement and reduce loss, leading to higher efficiencies and higher temperature operation of cascaded InAsSb lasers.

ACKNOWLEDGMENTS

We thank J. A. Bur for technical assistance. This work was supported by the U.S. Dept. of Energy under contract No. DE-AC04-94AL85000. Sandia is a multiprogram laboratory operated by Sandia Corporation for the United States Department of Energy.

REFERENCES

[1] A. A. Allerman, R. M. Biefeld, and S. R. Kurtz, Appl. Phys. Lett. **69**, 465 (1996).

[2] S. R. Kurtz, A. A. Allerman, and R. M. Biefeld, Appl. Phys. Lett. **70**, 3188 (1997).

[3] R. M. Biefeld, S. R. Kurtz, and A. A. Allerman, J. Electronic Mater., **26**, 903 (1997).

[4] J. Faist, F. Capasso, D. L. Sivco, C. Sirtori, A. L. Hutchinson, and A. Y. Cho, Science **264**, 553 (1994).

[5] R. Q. Yang, Superlatt. Microstruct. **17**, 77 (1995).

[6] J. R. Meyer, I. Vurgaftman, R. Q. Yang, and L. R. Ram-Mohan, Elect. Lett. **32**, 45 (1996).

[7] J. Faist, F. Capasso, C. Sirtori, D. L. Sivco, J. N. Baillargeon, A. L. Hutchinson, S. N. G. Chu, and A. Y. Cho., Appl. Phys. Lett. **68**, 3680 (1996).

[8] C. H. Lin, R. Q. Yang, D. Zhang, S. J. Murry, S. S. Pei, A. A. Allerman, and S. R. Kurtz, Elect. Lett. **33**, 598 (1997).

[9] R. Q. Yang, B. H. Yang, D. Zhang, C. H. Lin, S. J. Murry, H. Wu, and S. S. Pei, Appl. Phys. Lett. **71**, 2409 (1997).

[10] S. R. Kurtz, A. A. Allerman, R. M. Biefeld, and K. C. Baucom, Appl. Phys. Lett. **72**, 2093 (1998).

[11] W. G. Breiland and G. H. Evans, J. Electrochem. Soc., **138**, 1806 (1991).

[12] H.K. Choi and G.W. Turner, Appl. Phys. Lett. **67**, 332 (1995).

Figure Captions

Figure 1 - Band diagram of a multi-stage laser active region with compressed, type I InAsSb quantum wells separated by InAsP barriers, electron-hole generation by an InAs(n)/GaAsSb(p) semi-metal heterojunction, and an AlAsSb electron block

Figure 2. Effect of change in TBAs flow on the lattice match to the InAs substrate of an AlAsSb layer grown at 500 °C, 70 torr, a V/III ratio of 5.3, and a growth rate of 3.2 Å/s.

Figure 3. The composition variation of InAsSb and InAsP as a function of vapor phase composition under optimized growth conditions. (a) Dependence of Sb composition on the TESb/(TESb + TBAs) vapor phase composition. (b) Dependence of P composition on the variation of TBAs/(TBAs + Phosphine) vapor phase composition.

Figure 4. Comparison of the x-ray diffraction pattern of an InAsSb/InAs MQW laser structure grown in an MOCVD RDR(top pattern) versus the pattern for a MQW laser grown using a standard horizontal chamber configuration (bottom). The dotted line is a simulated x-ray spectrum for the RDR grown structure.

Figure 5. Comparison of the x-ray diffraction patterns for InAsSb/InAsP SLS's grown using identical growth conditions in (a), (b), and (c) but with the indicated purges between layers [(a) = 20 sec., (b) = 5 sec., and (c) = 0 sec.]. The sample in (d) was grown with a

slightly different composition than (c) with no purge time to achieve lattice matching with the InAs substrate.

Figure 6. X-ray diffraction pattern for a 10-stage, 5-well InAsSb/InAsP laser structure with 2 μm AlAsSb claddings and p-GaAsSb/n-InAs semi-metal heterojunction injection layers.

Figure 7. Laser emission spectra at 80 and 150 K for a 10-stage, 5-well laser with a 500 μm long stripe.

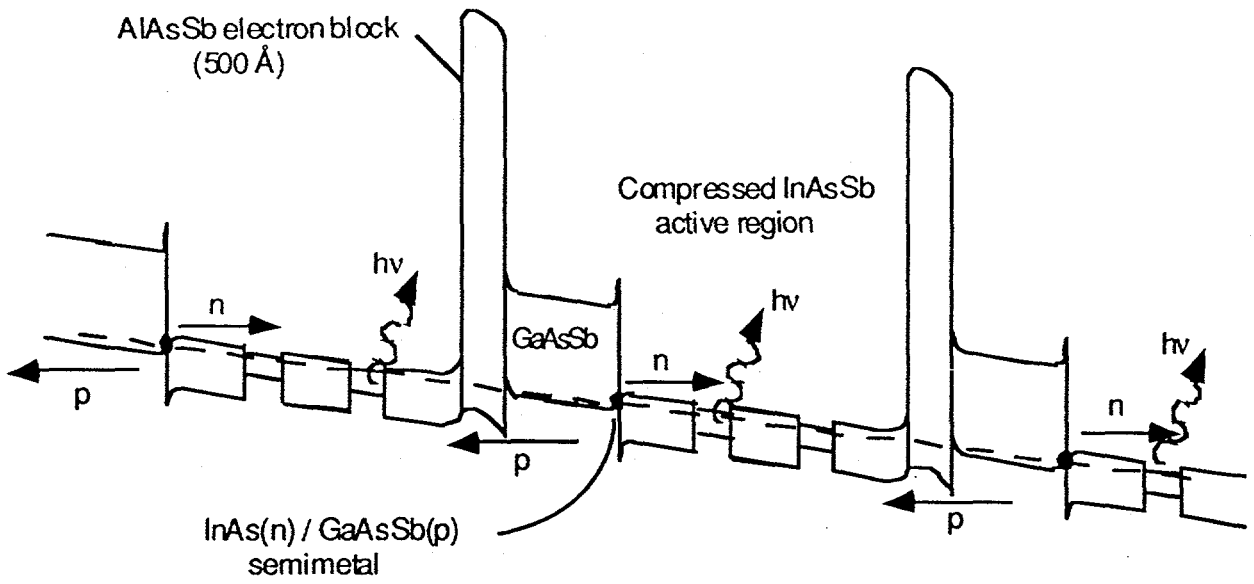

Figure 1 Biefeld et al.

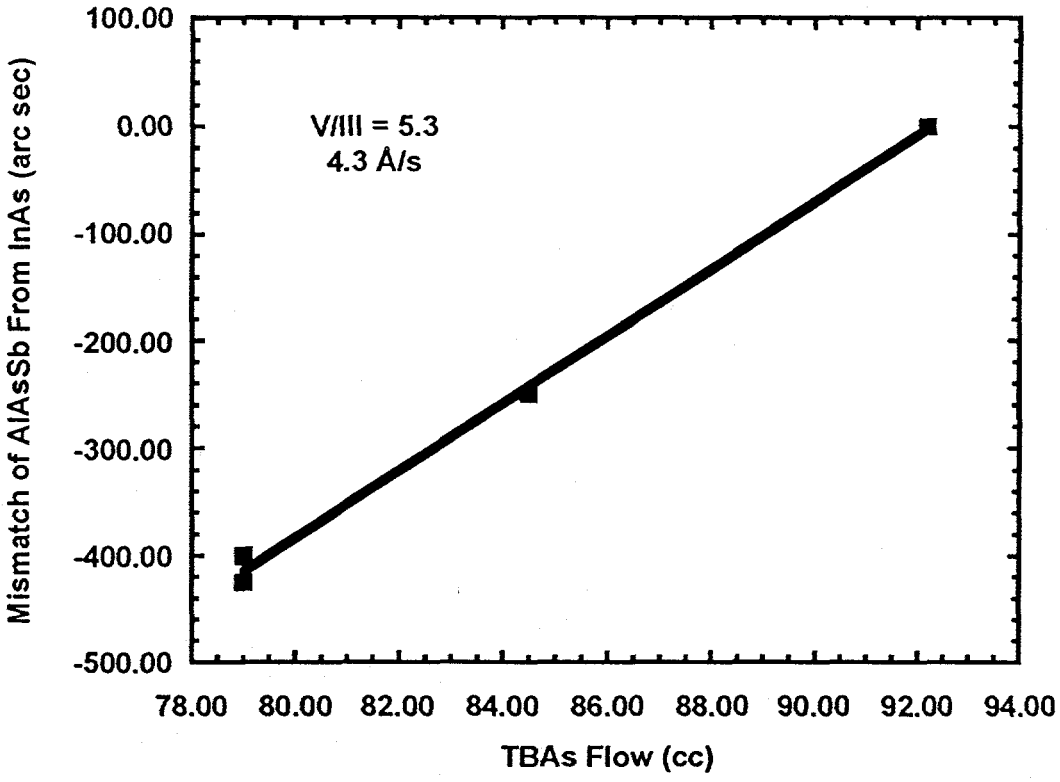

Figure 2. Biefeld et al.

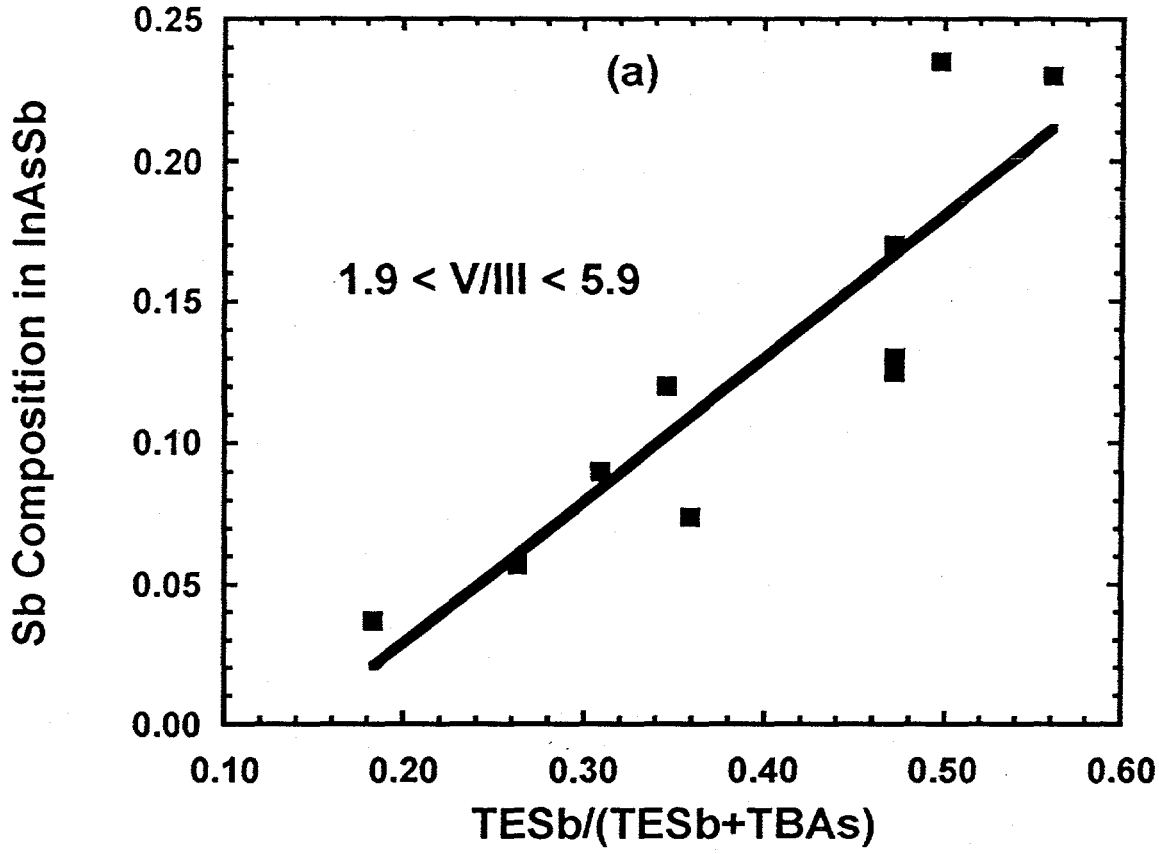

Figure 3a. Biefeld et al.

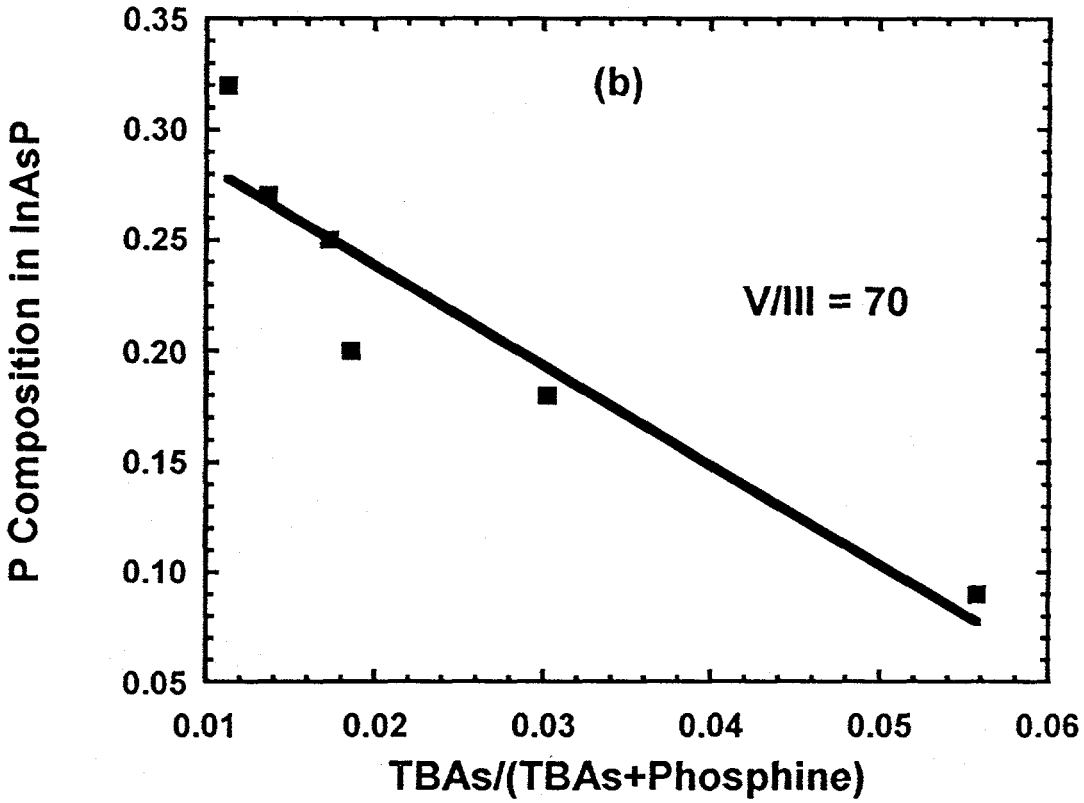

Figure 3b. Biefeld et al.

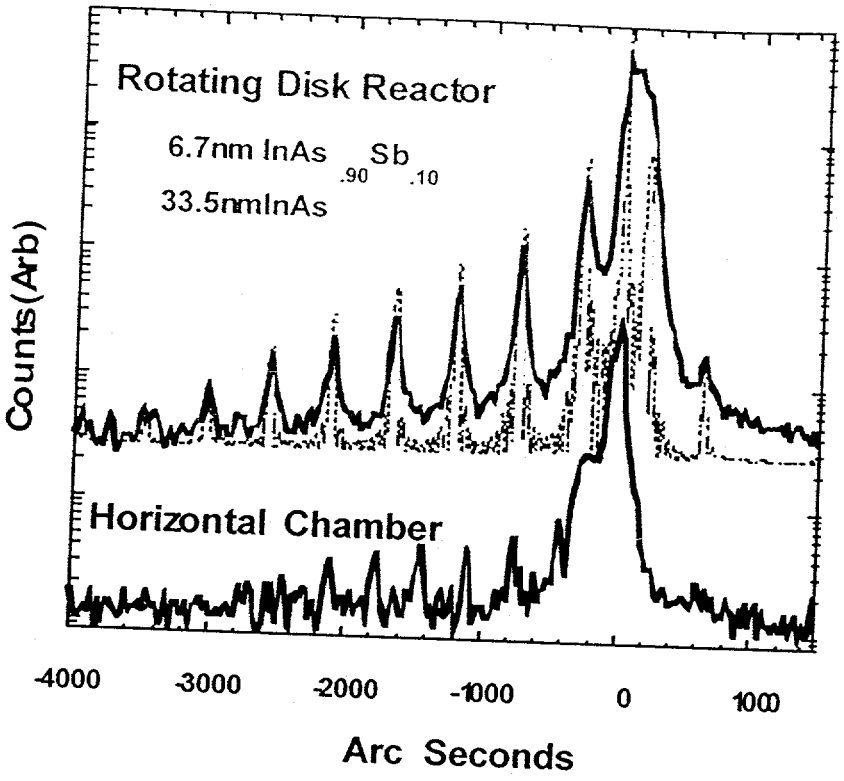

Figure 4. Biefeld et al.

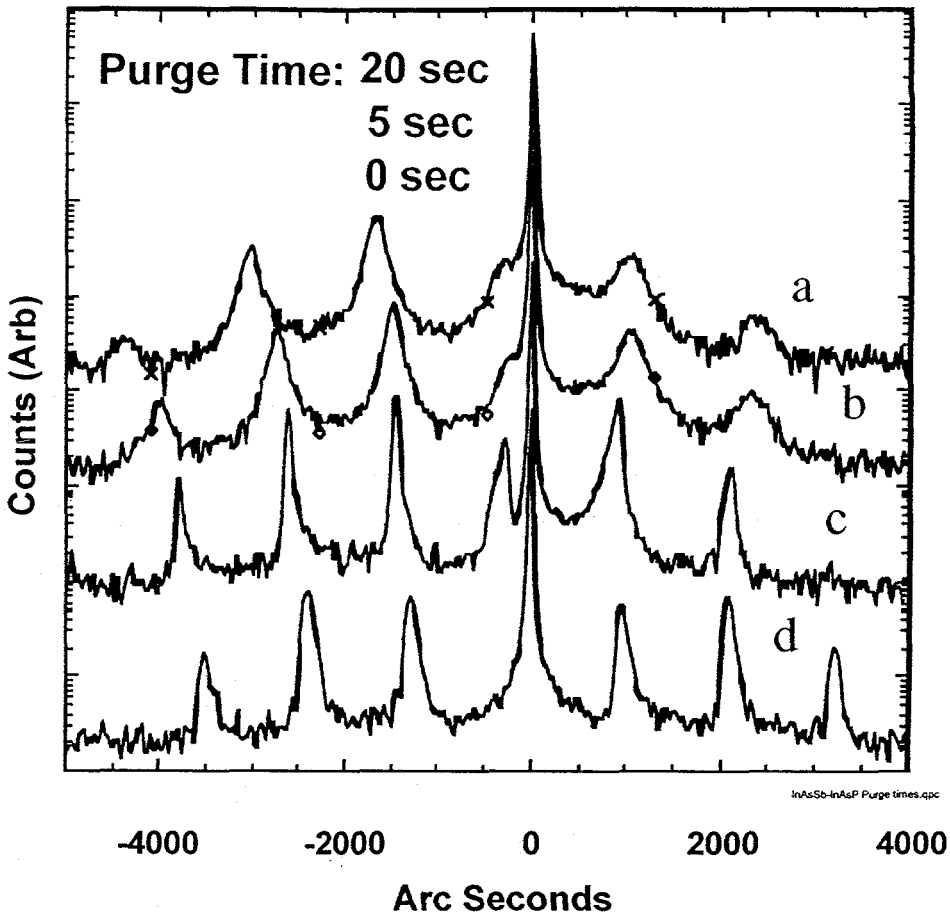

Figure 5. Biefeld et al.

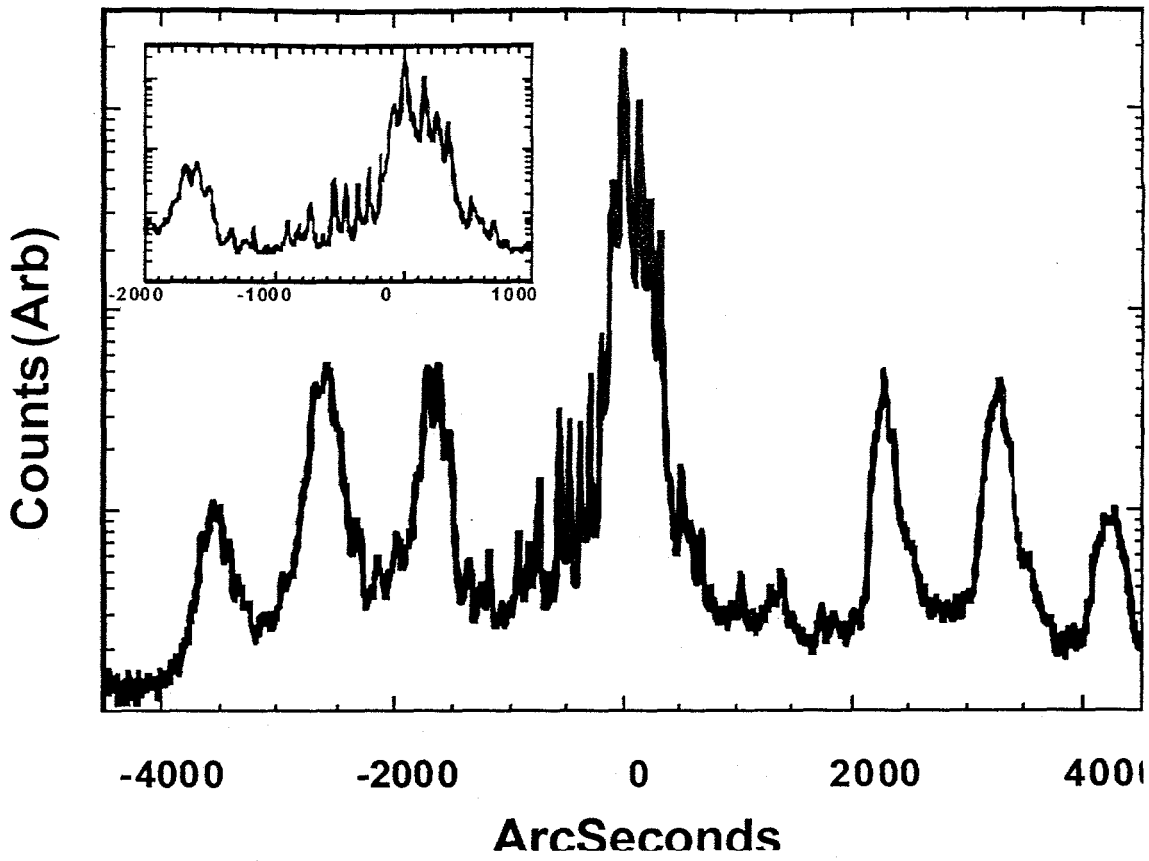

Figure 6. Biefeld et al.

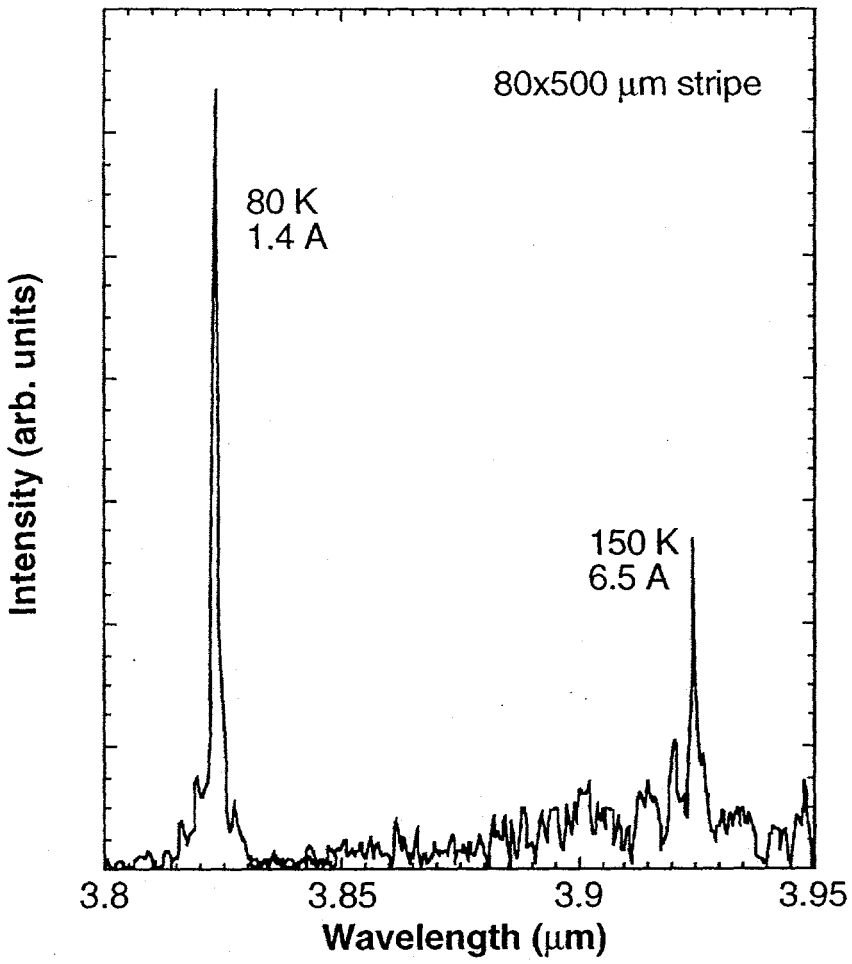

Figure 7. Biefeld et al.